Aalborg Universitet

A robust and fast generic voltage sag detection technique

L. Dantas, Joacillo; Lima, Francisco Kleber A.; Branco, Carlos Gustavo C.; Guerrero, Josep M.; Quintero, Juan Carlos Vasquez

Link to publication from Aalborg University

A ROBUST AND FAST GENERIC VOLTAGE SAG DETECTION TECHNIQUE

Joacillo. L. Dantas[1], Francisco Kleber A. Lima[1], Carlos Gustavo C. Branco[1], Josep M. Guerrero[2], Juan C. Vasquez[2]

[1]Departament of Electric Engineering,Federal University of Ceará, Fortaleza-Ceará, Brazil.

[2]Departament of Energy Technology, Aalborg University, Aalborg, Denmark.

joacillo@ifce.edu.br, klima@dee.ufc.br, gustavo@dee.ufc.br, juq@et.aau.dk, joz@et.aau.dk

Abstract - **In this paper, a fast and robust voltage sag detection algorithm, named VPS^{2}D, is introduced. Using the DSOGI, the algorithm creates a virtual positive sequence voltage and monitories the fundamental voltage component of each phase. After calculating the aggregate value in the $\alpha\beta$-reference frame, the algorithm can rapidly identify the starting and the ending of symmetric and asymmetric voltage sags, even if there are harmonics on the grid. Simulation and experimental results are given to validate the proposed algorithm.**

Keywords – **The author shall provide a maximum of 6 keywords (in alphabetical order) to help identify the major topics of the paper.**

I. INTRODUCTION

Voltage sag is one of the major factors that contribute to the power quality deterioration, and it is usually caused due to short circuits, overloads and high power motors starting [1]. Applying the concept of aggregate voltage, first introduced in [2], it is not difficult to identify symmetric voltage sag. However the most of the voltage sags are asymmetric, and more than 75% of them are single-phase voltage sags [1]. This fact has encouraged researches concerned with unbalanced voltage sag detection as in [3], where a nonlinear adaptive filter was used in order to track the amplitude of the sag. However, the proposed technique was not tested under distorted conditions.

A synchronous rotating reference frame combined with a differentiator and a low pass filter was used in [4] to detect voltage sags. The differentiator was influenced by harmonics, In [5], an improvement of their previous work has been presented, although it was used 0 pu voltage in the experimental results; that is not voltage sag but rather an interruption.

The work developed in [6] regards to combine the dq positive and negative sequence components, from a three-phase system, in a linear relationship. The recursive discrete Fourier transformer extracted the magnitude of the components. The detection time for symmetric and asymmetric sags was 6.6 ms, and 4 ms respectively.

Using the measurements of line currents, the study in [7] proposed a technique for detecting sources of voltage sags. Change in the magnitude and phase of the instantaneous positive-sequence current was the criterion for proposed technique

The voltage sags have a negative influence in wind power generators connected to the grid, especially in the Doubly Fed Induction Generator, because this machine has the stator circuit direct connected to the grid [8] [9]. Take into account the dynamic voltage restorer (DVR) to improve the LVRT capability for wind power generators [10], [11], [12], [13], [14], and the new grid codes and their LVRT requirements for wind power system [15], [16], it is mandatory an accurate and fast voltage sag detection system that can be used for the DVR to help the wind turbine to overcome this stressful mishap.

This paper addresses the design and implementation of a rapid and robust voltage sag detection algorithm named VPS^2D, that stands for Virtual Positive Sequence Sag Detection. It creates a virtual positive sequence voltage in the $\alpha\beta$ reference frame, and also monitors the fundamental component of the voltage for each phase. The VPS^2D is able to quickly and accurately detect symmetric and asymmetric voltage sags, even within distorted voltage systems. Simulation and experimental results are shown to validate the proposed algorithm.

The remainder of this paper is organized as follows: In section II, the voltage sag detection algorithm is explained. Simulation and experimental results are given in sections III and IV respectively. Section V concludes this paper.

II. ALGORITHM DESCRIPTION

Considering an ABC three-phase voltage system from the grid, denoted by $v_a(t)$, $v_b(t)$ and $v_c(t)$. Delaying the voltage $v_a(t)$ of a quarter of the period T, it is possible to obtain $v_{a\frac{\pi}{2}}(t)$. The voltages $v_{a\alpha}(t) = v_a(t)$ and $v_{a\beta}(t) = v_{a\frac{\pi}{2}}(t)$ comprise a single-phase voltage system in the $\alpha\beta$ reference frame.

The Dual Second Order Generalized Integrator Frequency-Locked Loop (DSOGI-FLL) is a grid voltage synchronization method that uses an adaptive-frequency track structure [17]. Deploying the voltages $v_{a\alpha}(t)$ and $v_{a\beta}(t)$ as inputs of the DSOGI-FLL it generates four outputs that are $v'_{a\alpha}(t)$, $qv'_{a\alpha}(t)$, $v'_{a\beta}(t)$ and $qv'_{a\beta}(t)$. The VPS^2D, by using the output signals, extracts the virtual positive sequence voltages. Indeed, there is no real positive or negative sequence in a single-phase system. Therefore, these voltages were named as virtual positive sequence voltages. The equations 1 and 2 show the components α and β for the virtual positive sequence voltages in the phase A. The algorithm implements three DSOGI-FLLs, one for each phase.

$$v_{a\alpha}^+(t) = v'_{a\alpha}(t) - qv'_{a\alpha}(t), \qquad (1)$$

$$v_{a\beta}^{+}(t) = q v_{a\alpha}'(t) + v_{a\beta}'(t) \cdot \qquad (2)$$

Where $q = e^{-j\frac{\pi}{2}}$ is a $\frac{\pi}{2}$ radians phase-shift operator. Adopting the same procedure for phases B and C, the virtual positive sequence voltage components are $v_{b\alpha}^{+}(t)$, $v_{b\beta}^{+}(t)$, $v_{c\alpha}^{+}(t)$ and $v_{c\beta}^{+}(t)$. It is important to highlight that the filtering characteristic of the DSOGI attenuates the effect of the harmonics from input to the output [16], [17],i.e., the virtual positive sequence voltages are sinusoidal or quasi-sinusoidal wave forms, even if the original three-phase system contains harmonic components. The block diagram illustrating the extraction of the virtual positive sequence components from phase A is depicted in Figure 1, assuming that ω' is the angular frequency of grid voltage system tuned by the FLL, and the division by $\sqrt{2}V_{aRMS}$ is used to represent the maximum value V_{aMax}^{+} of $v_{a\alpha}^{+}(t)$ and $v_{a\beta}^{+}(t)$ in per unit. V_{aRMS} represents the root mean square value of the phase-A voltage. The circuit is repeated for the others phases. Similarly, the maximum values for the phases B and C are V_{bMax}^{+} and V_{cMax}^{+}.
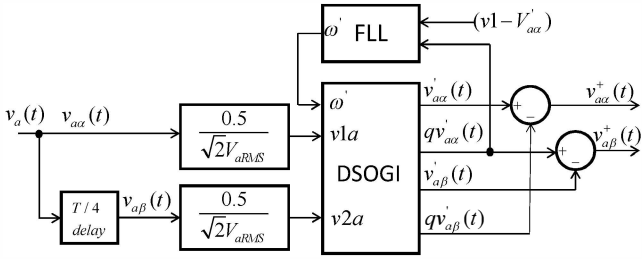

Fig. 1. Extraction of the virtual positive sequence components of the phase A.

The aggregate voltage for the virtual positive sequence in the $\alpha\beta$ reference frame, from now on called aggregated voltage, can be written as

$$V_{a\alpha\beta Agg}^{+} = \sqrt{v_{a\alpha}^{+}(t)^2 + v_{a\beta}^{+}(t)^2}, \qquad (3)$$

$$V_{a\alpha\beta Agg}^{+} = \sqrt{[V_{aMax}^{+} sen(\omega t)]^2 + [V_{aMax}^{+} cos(\omega t)]^2}, \qquad (4)$$

$$V_{a\alpha\beta Agg}^{+} = V_{aMax}^{+}. \qquad (5)$$

Considering the phases B and C, the aggregate voltages are determined by the equations (6) and (7).

$$V_{b\alpha\beta Agg}^{+} = \sqrt{v_{b\alpha}^{+}(t)^2 + v_{b\beta}^{+}(t)^2} = V_{b\alpha\beta Agg}^{+}, \qquad (6)$$

$$V_{c\alpha\beta Agg}^{+} = \sqrt{v_{c\alpha}^{+}(t)^2 + v_{c\beta}^{+}(t)^2} = V_{c\alpha\beta Agg}^{+}. \qquad (7)$$

Voltage sag in one phase makes the corresponding aggregate value become less than 1pu, hence the algorithm can easily identify single-phase, two-phase and three-phase voltage sags as shown in Figure 2.
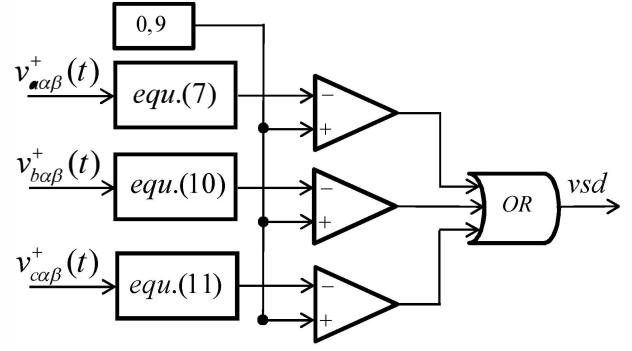

Fig. 2. The sag detection circuit.

III. SIMULATION STUDIES

In order to confirm the efficiency of the algorithm, simulations were carried out on MATLAB/Simulink environment.

A. Single-Phase Sag Simulation

Figure 3 and 4 show the voltage dip, the vsd signal and the aggregate voltage for 0.4 pu single-phase voltage sag. The aggregate voltage of the phases B and C were not affected ($V_{b\alpha\beta Agg}^{+} = V_{c\alpha\beta Agg}^{+} = 1$). The algorithm took 3.8 ms to detect the single-phase voltage.
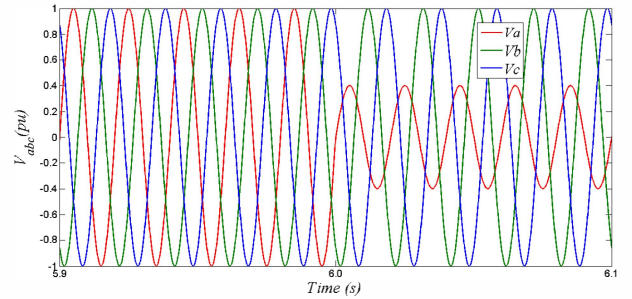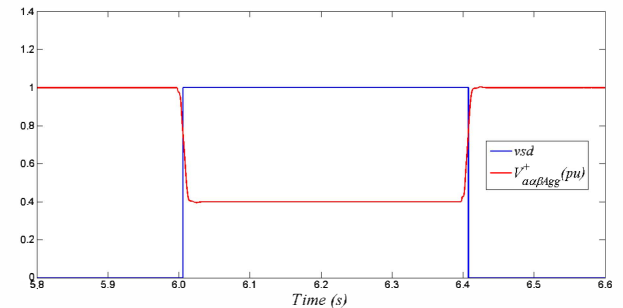

Fig. 3. Single-phase voltage sag (0.4 pu.)

Fig. 4. The voltage sag detection signal (vsd) and the aggregate voltage of the phase A.

B. Two-Phase Sag Simulation

It was provoked 0.6 pu voltage sag in the phases A and B (Figure 5). Figure 6 depicted the voltage sag detection signal (vsd) and the the aggregate voltage for the phase B.
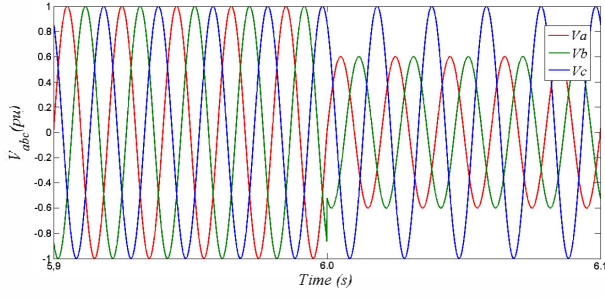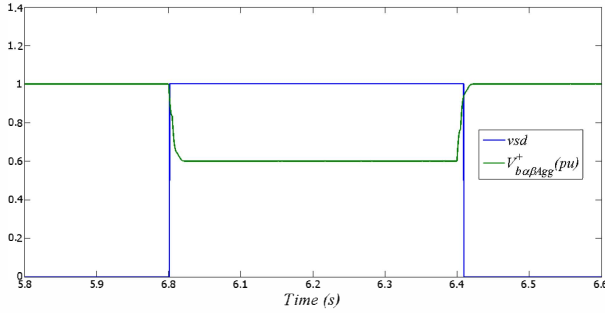
Fig. 5. Two-phase voltage sag (0.6 pu).

Fig. 6. The voltage sag detection signal (vsd) and the aggregate voltage of the phase B.

IV. EXPERIMENTAL RESULTS

The performance of the proposed generic voltage sag detection algorithm was tested in a power electronic setup acting as a grid simulator. It generates the voltage sags and distortions required for the experiment.

A. Grid Simulator

The Grid Simulator was first presented in [18]. It consists of two inverters in back-to-back topology with a LCL input filter and a LC output filter. It can produce voltage disturbances as sags, swells, flickers, and harmonic distortions. A dSPACE 1006 allows the real-time management of the VPS^2D algorithm. The experiment was carried out in the Microgrid research laboratory . The experimental setup can be seen in Figure 7. Figure 8 shows the scheme of the Grid Simulator integrated with the dSPACE and the proposed algorithm.
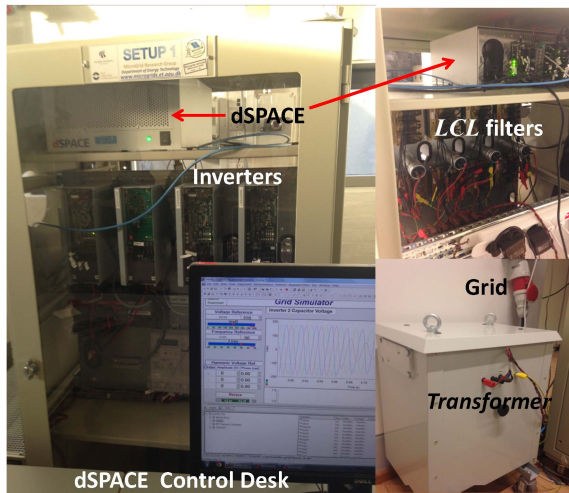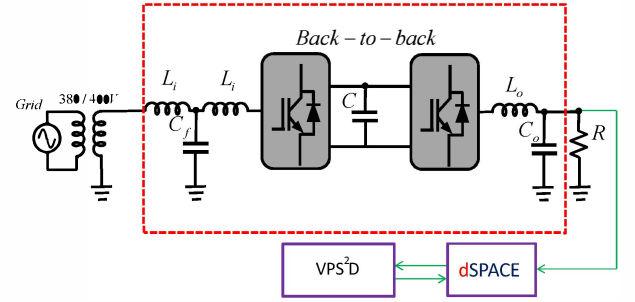

Fig. 7. Experimental setup.

Fig. 8. Scheme of the grid simulator.

The reference voltages needed to produce the sags in the grid simulator are expressed in the $\alpha\beta$ reference frame. Neglecting the zero sequence components, the inverse of the Clarke transformation is derived as

$$v_{a_{Ref}}(t) = \sqrt{\frac{2}{3}} k_1 \sqrt{2} V_{\alpha rms} cos(\omega t), \qquad (8)$$

$$v_{b_{Ref}}(t) = -\frac{k_1 \sqrt{2} V_{\alpha rms} cos(\omega t)}{\sqrt{6}} + k_2 V_{\beta rms} sin(\omega t), \quad (9)$$

$$v_{c_{Ref}}(t) = -\frac{k_1 \sqrt{2} V_{\alpha rms}(t)}{\sqrt{6}} - k_2 V_{\beta rms} sin(\omega t)\cdot \qquad (10)$$

Where the subscript Ref stands for reference signal. The real variables $k1$ and $k2$ are used to produce the desired voltage sags. $V_{\alpha rms}$ and $V_{\beta rms}$ are the root mean square of the rated voltage of the system.

A. Single-Phase Voltage Sag

Setting $k1 = 0.4$ and $k2 = 1$ the result is 0.4 pu voltage sag on phase A. But according to equations (8), (9) and (10), it also provoke 0.89 pu voltage sag on phases B and C (Figure 9). Figure 10 shows the vsd signal. The sag length of time was 392 ms and the detection time for this fault was 5 ms (Figure 11). The relationship between the virtual positive aggregate voltage of the phase A and the vsd signal is highlighted in Figure 12.
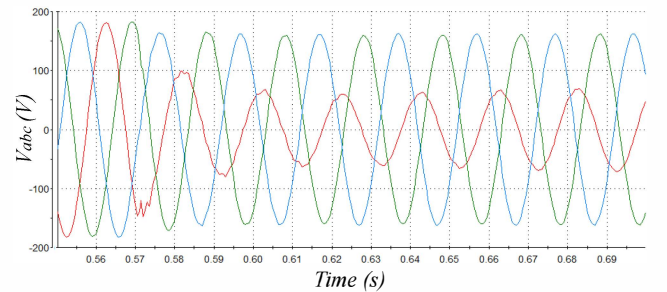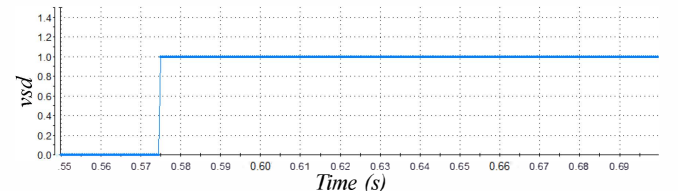

Fig. 9. 0.4 pu single-phase voltage sag.

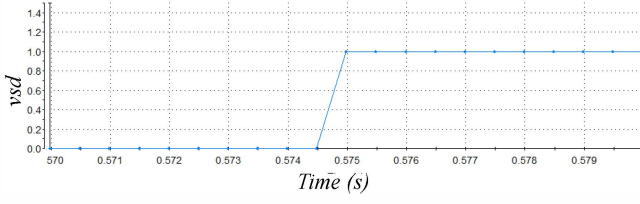
Fig. 10. The voltage sag detection signal (vsd).

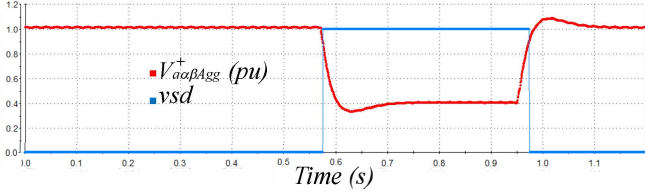Fig. 11. Sag detection time (5ms).

Fig. 12. The vsd signal and the aggregate voltage of the phase A.

B. *Single-phase Voltage Sag in a Three-phase Distorted System*

Due to the proliferation of non-linear loads, voltage distortions have become a common problem in distribution network [19] as well as voltage sags in a distorted voltage system. This proposed algorithm also works under harmonic voltage conditions.

A distorted three-phase voltage system composed by 10% of 5th, 5% 0f 7th and 3% of 11th harmonics was produced by the grid simulator. The generated distortion is much more severe than the limits for harmonics outlined by IEEE standard 519-1992 [20]. Figures 13 and 14 show the voltage sag, vsd signal and the $\alpha\beta$-aggregate voltage of the phase A.
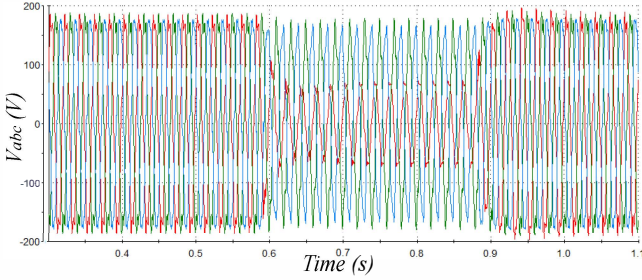

Fig. 13. Detection time of the single-phase voltage sag.
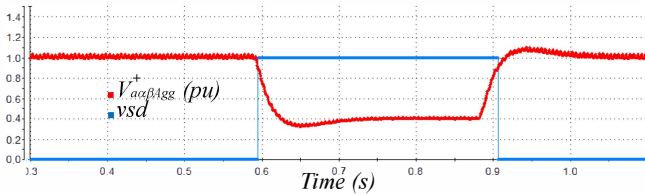

Fig. 14. The voltage sag detection signal (vsd) and the aggregate voltage of the phase A.

The signals $v1a$ and $v2a$, previously showed on Figure 1, contain the information about voltage harmonics on phase A. When the voltage on phase A, B or C drops each harmonic component decreases in the same proportion. The VPS^2D needs to monitor only the virtual positive sequence of the fundamental component. This characteristic of the algorithm permits sag identification under harmonic conditions without trip-

ping the output vsd signal. It is possible to observe the distorted voltage of the system in Figure 15. Figure 16 depicts the distorted $v1a$ voltage and the virtual positive sequence voltage $v_{a\alpha}^+$ that present $THD = 11.58\%$ and $THD = 1.73\%$ respectively.
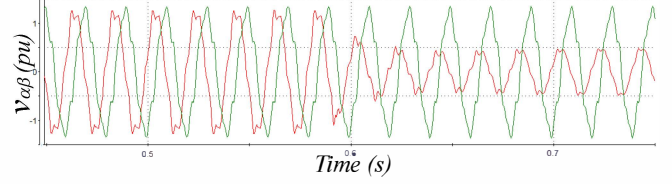

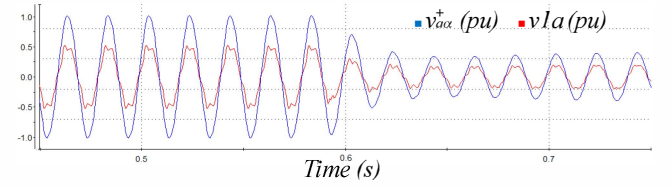Fig. 15. Voltages of the system in the $\alpha\beta - reference frame$.

Fig. 16. The virtual positive sequence voltage of the phase A and $v1a$.

C. *Two-Phase Voltage Sag*

Phase-to-Phase and Phase-to-Phase-to-Ground are types of two-phase voltage sags, and they represent 20% of the sag stochastic prediction [1]. The grid simulator produced 0.6 pu phase-to-phase-to-ground voltage sag in the phases B and C. The final instants of the voltage sag as well the vsd signal detecting the ending of the sag are depicted in Figures 17 and 18.
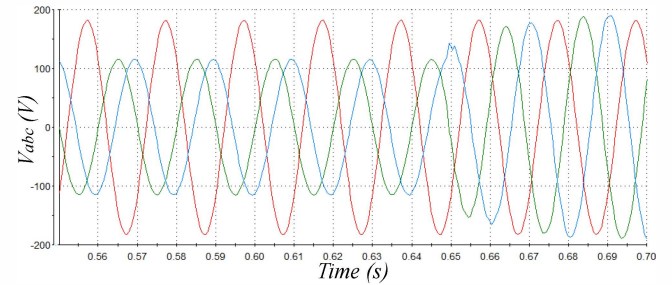
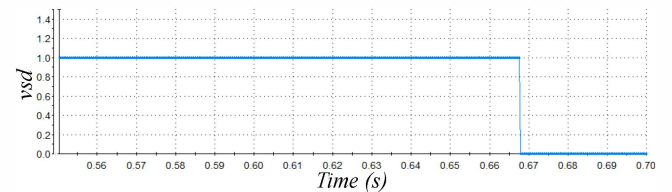

Fig. 17. The final instants of the two-phase voltage sag.

Fig. 18. vsd signal detecting the ending of the sag.

D. *Three-Phase Voltage Sag*

Representing less than 5% of the sag occurrences [1], the three-phase is the most uncommon type of sag. In order to evaluate the performance of the proposed algorithm under this type of fault, 0.3 pu balanced voltage sag was generated by the grid simulator during 300 ms as depicted in Figure 19.

During this contingency the voltage of each phase drops simultaneously. The expected 0.3 pu for the aggregate voltages $V_{a\alpha\beta Agg}^+$, $V_{b\alpha\beta Agg}^+$ and $V_{c\alpha\beta Agg}^+$ are confirmed by experimental results, as illustrated in Figures 20, 21 and 22. The sag detection signal is also depicted in Figure 22.
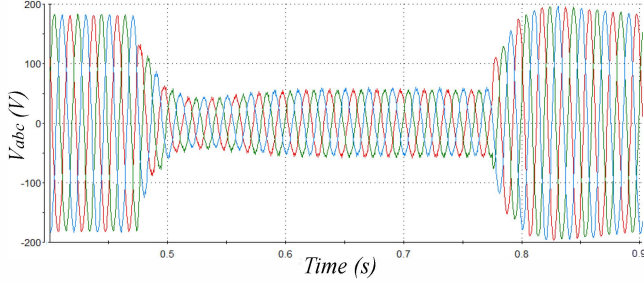

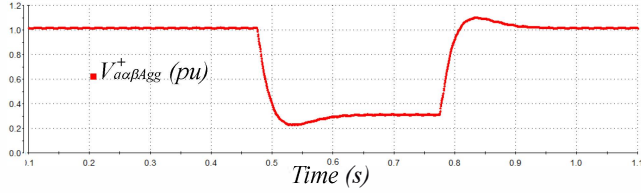Fig. 19. Three-phase voltage sag.

Fig. 20. Aggregated voltage of the phase A ($V_{a\alpha\beta Agg}^+$).
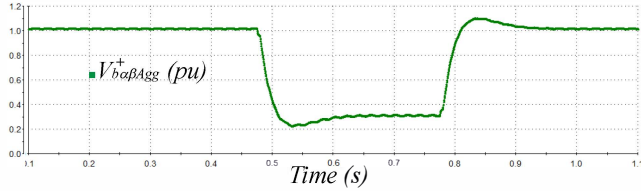

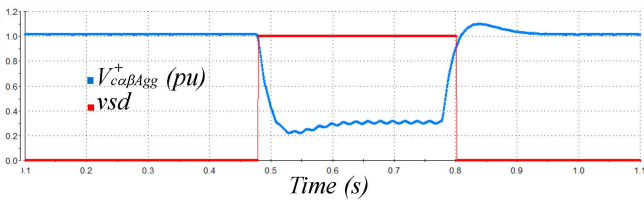Fig. 21. Aggregated voltage of the phase A ($V_{b\alpha\beta Agg}^+$).

Fig. 22. The vsd signal and the aggregated voltage of the phase A ($V_{c\alpha\beta Agg}^+$).

E. Balanced Voltage Sag in a Distorted System

In this experiment, the grid simulator came up with three-phase voltage system comprised by 10% of 7th harmonic and 5% of 11th harmonic, and given rise a 0.3 pu balanced voltage sag during 300 ms (Figure 23). For this case, the aggregate voltage for each phase has the same wave form. The sag detection signal is shown in Figure 24.
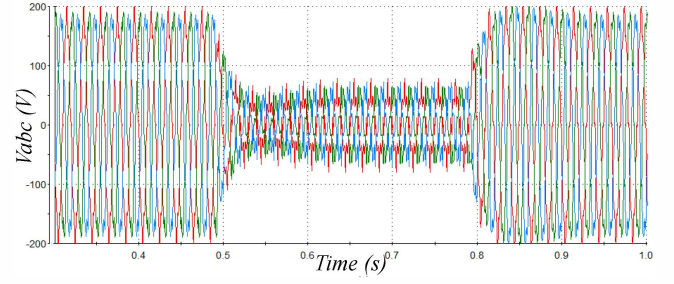

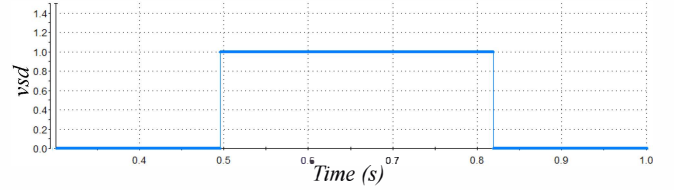Fig. 23. Distorted balanced voltage sag (7th and 11th harmonics).

Fig. 24. The voltage sag detection in a distorted system.

It is possible to observe the presence of harmonics on the $\alpha\beta$ reference frame, Figure 25. The virtual positive sequence voltages for each phase do not present harmonics, as shown in Figures 26, 27 and 28.
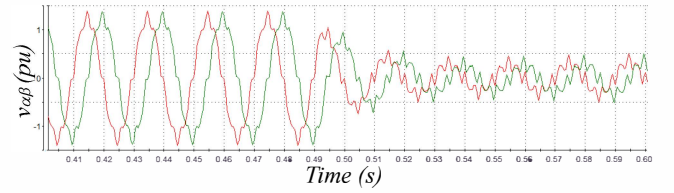

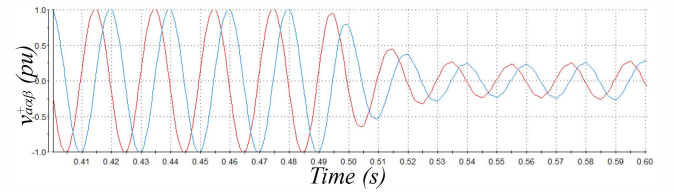Fig. 25. The three-phase voltage in the $\alpha\beta$-reference .

Fig. 26. Virtual positive sequence voltages in the phase A ($v_{a\alpha}^+, v_{a\beta}^+$).
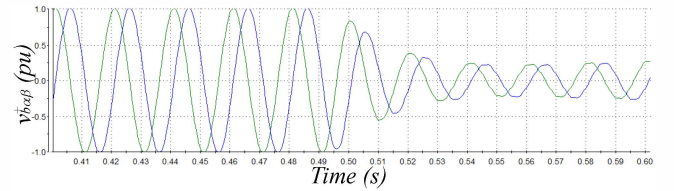

Fig. 27. Virtual positive sequence voltages in the phase B ($v_{b\alpha}^+, v_{b\beta}^+$).
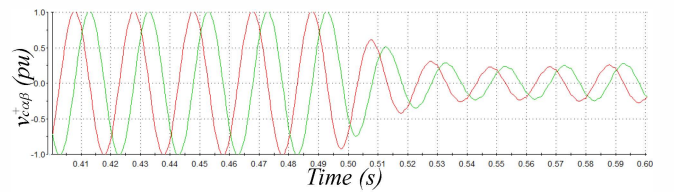

Fig. 28. Virtual positive sequence voltages in the phase C ($v_{c\alpha}^+, v_{c\beta}^+$).

The sag detection times for simulations and experiments are in tables I. The detection time in the simulation is smaller than in the experiment due to the analogue to digital conversion delay.

TABLE I
Sag detection time.

	Sag :0.4 pu	
Tipo	**Simulation**	**Experiment**
Single-phase	3,8 ms	5,0 ms
Two-phase	1,1 ms	4,9 ms
Three-phase	1,1 ms	4,9 ms

V. CONCLUSION

A rapid and generic voltage sag detection algorithm, named VPS^2D, has been proposed in this paper. It is able to detect, fast and accurately, all kind of voltage sags. The virtual positive sequence voltage, created by the algorithm, made it also suitable for distorted conditions. The grid simulator, presented in [18], accomplished the voltage sags required for the validation. Experimental results have confirmed the effectiveness and robustness of the proposed algorithm

ACKNOWLEDGEMENT

REFERENCES

[1] J.A. Martinez and J. Martin-Arnedo. Voltage sag studies in distribution networks - part ii: voltage sag assessment. *IEEE Transactions on Power Delivery*, 21(3):1679–1688, July 2006.

[2] F. Buchholz. *Die drehstrom-scheinleistung bei ungleichmäßiger belastune der drei zweige*, volume 2. Licht und Kraft, Zeitschrift fü Elekt., 1922.

[3] R. Naiddo and P. Pillay. A new method of voltage sag and swell detection. *IEEE Transactions on Power Delivery*, 22(2):1056–1063, April 2007.

[4] Y. Sillapawicharm and Y. Kumsuwan. An improvement of synchronously rotating reference frame based voltage sag detection for voltage sag compensation applications under distorted grid voltages. In *IEEE Power Electronics and Drive Systems (PEDS)- Ninth International Conference*, pages 100–103, July 2011.

[5] Y. Kumsuwan and Y. Sillapawicharm. A fast synchronously rotating reference frame-based voltage sag detection under practical grid voltages for voltage sag compensation systems. In *IET 6th conference- Power Electronics, Machines and Drives (PEMD 2012)*, pages 1–5, March 2012.

[6] S. Zhou, J.Liu, L. Zhou, Z. Yangquer, and Y. Xu. Sag detection algorithm for dynamic voltage restorer used in wind farms under unbalanced and distorted grid voltage conditions. In *IEEE ECCE Asia Downunder)*, pages 601–606, June 2013.

[7] B. Polajzer, G. Stumberger, and D.Dolinar. Instantaneous positive-sequence current applied for detecting voltage sag source. *IET Generation, Transmission Distribution*, 9(4):319–227, 2015.

[8] Z. Chen, J.M. Guerrero, and F. Blaaljerg. A review of the state of the art of power electronics for wind turbines. *IEEE Transactions on Power Electronics*, 24(8):1859–1875, August 2009.

[9] F.K.A. Lima, E.H. Watanabe, P.Rodriguez, and A. Luna. Controle de gerador de indução duplamente alimentado diante de afundamentos de tensão. *SOBRAEP*, 14(3):189–199, August 2009.

[10] P. S. Flannery and G. Venkataramanan. Unbalanced voltage sag ride-through of a doubly fed generator wind turbine with series grid-side converters. *IEEE Transactions on Industrial Applications.*, 45(5):1879–1887, September 2009.

[11] C. Wessels, F. Gebhardt, and W. F. Funchs. Fault ride-through technique of a dfig wind turbine using dynamic voltage restorer during symmetric and asymmetric grid faults. *IEEE Transactions on Power Electronics.*, 26(3):807–815, March 2011.

[12] A. O. Ibrahim, T.H Nguyen, D.C Lee, and K. Su-Chang and. A fault ride-through technique of dfig wind turbine systems using dynamic voltage restorer. *IEEE Transactions on Energy Conversion.*, 26(3):871–882, September 2011.

[13] A. Roln, F. Crcoles, and J. Pedra. Behaviour of the doubly fed induction generator exposed to unsymmetrical voltage sags. *IET Electric Power Application.*, 6(8):561–574, 2012.

[14] F.L.A. Jowder. Design and analysis of dynamic voltage restorer for deep voltage sag and harmonic compensation. *IET Generation, Transmission Distribution*, 3(6):547–560, 2009.

[15] M. Tsili and S. Papathanassiou. A review of grid code technical requirements for wind farms. *IET Renew Power Generation*, 3(3):308–332, 2009.

[16] R. Teodoresco, M. Liserre, and P. Rodriguez. *Grid Converter for Photovoltaic and Wind Power Systems*. John Wiley & Sons, Inc., 2011.

[17] P. Rodriguez, A. Luna, and M. Ciobotaru and. Advanced grid synchronization system for power converters under unbalanced and distorted operating conditions. In *IEEE Industrial Electronics, IECON - 32nd Annual Conference*, pages 5173–5178, November 2006.

[18] J. Eloy-Garcia, J. C. Vasquez, and J. M. Guerrero. Grid simulator for power quality assessment of micro-grids. *IET Power Electronics*, 6(4):700–709, 2013.

[19] X. Wang, J. M. Guerrero, F. Blaabjerg, and Z. Chen. Secondary voltage control for harmonics suppression in islanded microgrids. In *IEEE Power and Energy Society General Meeting)*, pages 1–8, July 2011.

[20] IEEE. Std 519-1992. pages 84–87, 1993.